

Hepatocyte Nuclear Factor 4 α Controls Iron Metabolism and Regulates Transferrin Receptor 2 in Mouse Liver*

Received for publication, September 25, 2015, and in revised form, October 30, 2015. Published, JBC Papers in Press, November 2, 2015, DOI 10.1074/jbc.M115.694414

Shunsuke Matsuo[‡], Masayuki Ogawa[‡], Martina U. Muckenthaler[§], Yumiko Mizui[‡], Shota Sasaki[‡], Takafumi Fujimura[‡], Masayuki Takizawa[‡], Nagayuki Ariga[‡], Hiroaki Ozaki[‡], Masakiyo Sakaguchi[¶], Frank J. Gonzalez^{||}, and Yusuke Inoue^{‡1}

From the [‡]Division of Molecular Science, Graduate School of Science and Technology, Gunma University, Kiryu, Gunma 376-8515, Japan, the [§]Department of Pediatric Oncology, Hematology and Immunology, University of Heidelberg, 69120 Heidelberg, Germany, the [¶]Department of Cell Biology, Okayama University Graduate School of Medicine, Dentistry, and Pharmaceutical Sciences, Okayama 700-8558, Japan, and the ^{||}Laboratory of Metabolism, Center for Cancer Research, NCI, National Institutes of Health, Bethesda, Maryland 20852

Iron is an essential element in biological systems, but excess iron promotes the formation of reactive oxygen species, resulting in cellular toxicity. Several iron-related genes are highly expressed in the liver, a tissue in which hepatocyte nuclear factor 4 α (HNF4 α) plays a critical role in controlling gene expression. Therefore, the role of hepatic HNF4 α in iron homeostasis was examined using liver-specific HNF4 α -null mice (*Hnf4a* ^{Δ H} mice). *Hnf4a* ^{Δ H} mice exhibit hypoferremia and a significant change in hepatic gene expression. Notably, the expression of transferrin receptor 2 (*Tfr2*) mRNA was markedly decreased in *Hnf4a* ^{Δ H} mice. Promoter analysis of the *Tfr2* gene showed that the basal promoter was located at a GC-rich region upstream of the transcription start site, a region that can be transactivated in an HNF4 α -independent manner. HNF4 α -dependent expression of *Tfr2* was mediated by a proximal promoter containing two HNF4 α -binding sites located between the transcription start site and the translation start site. Both the GC-rich region of the basal promoter and the HNF4 α -binding sites were required for maximal transactivation. Moreover, siRNA knockdown of HNF4 α suppressed *TFR2* expression in human HCC cells. These results suggest that *Tfr2* is a novel target gene for HNF4 α , and hepatic HNF4 α plays a critical role in iron homeostasis.

Iron is an essential metallic element in living organisms and is required for the transport of oxygen by hemoglobin in red blood cells and for redox reactions by catalase and various cytochrome P450s. Because most of the iron in the human body is contained in hemoglobin and is recycled from aged red blood cells in the reticuloendothelial system, only 1–2 mg of iron are absorbed at the duodenum, and the amount exactly matches

that of iron loss (1, 2). Iron deficiency causes anemia, whereas iron overload has a cytotoxic effect due to the production of reactive oxygen species (ROS).² Thus, the amount of iron in the organism must be tightly regulated by various processes such as absorption, transport, cellular uptake, and storage (1–3).

Liver is the most important organ for iron metabolism, and many iron-related genes encoding transferrin (TF), transferrin receptor 2 (TFR2), and hepcidin (HAMP), for example, are highly expressed in hepatocytes. TF is a plasma iron carrier, and iron-loaded TF is mainly endocytosed into most tissues through transferrin receptor 1 (TFR1) (2–4). Congenital apo-transferrinemia, deficiency of serum TF, causes iron deficiency anemia (5). Unlike TFR2, TFR1 is ubiquitously expressed in many tissues and is required for iron delivery to cells (4, 6). Mutations of the *TFR2* gene cause iron overload disease, hereditary hemochromatosis, and the affinity of TFR2 to holo-TF was 25-fold lower when compared with that of TFR1, indicating that TFR2 functions as an iron sensor unlike TFR1 (7–9). TFR2 is also an upstream regulator of HAMP, a peptide hormone secreted from liver (10). HAMP binds to iron exporter, ferroportin 1 (FPN1), and induces internalization and degradation of FPN1, resulting in decreased efflux of iron from the duodenum (11). In addition to the *TFR2* gene, mutations of the *HAMP* and *FPN1* genes also cause hereditary hemochromatosis (12). Thus, the HAMP-FPN1 axis is a central coordinator and an iron sensor in the body. Agonists and antagonists of these factors, including HAMP, are under development as therapeutic targets for iron overload disease and anemia of inflammation (1).

HNF4 α is an orphan member of the nuclear receptor superfamily and positively regulates many genes involved in liver-specific functions (13, 14). HNF4 α was shown to transactivate at the *TF* gene through an HNF4 α -binding site within the promoter region in the human hepatoma cell line (15). Moreover, an HNF4 α -binding site in the *Hamp* promoter was essential for bone morphogenetic protein- and hemojuvelin-induced transactivation (16), and hepatic expression of *Hamp* mRNA was increased in liver-specific *Hnf4a*-null (*Hnf4a* ^{Δ H}) mice (17). These results suggest that hepatic HNF4 α could be involved in the control of iron metabolism through these target genes, but

* This work was supported in part by grants from the Ministry of Education, Culture, Sports, Science, and Technology of Japan Grant-in-aid for Scientific Research 25460490 (to Y. I.) and Kato Memorial Bioscience Foundation (to Y. I.). The authors declare that they have no conflicts of interest with the contents of this article. The content is solely the responsibility of the authors and does not necessarily represent the official views of the National Institutes of Health.

✂ Author's Choice—Final version free via Creative Commons CC-BY license.

¹ To whom correspondence should be addressed: Division of Molecular Science, Graduate School of Science and Technology, Gunma University, 1-5-1 Tenjin-cho, Kiryu, Gunma 376-8515, Japan., Tel./Fax: 81-277-30-1431; E-mail: yinoue@gunma-u.ac.jp.

² The abbreviations used are: ROS, reactive oxygen species; HNF4 α , hepatocyte nuclear factor 4 α ; TUBG, γ -tubulin; TF, transferrin.

Regulation of *Tfr2* by Hepatic HNF4 α

the *in vivo* relationship between HNF4 α and iron metabolism in adult liver has not been explored. Because *Hnf4a*^{ΔH} mice exhibit many phenotypes that attenuate liver-specific functions such as lipid and ammonia metabolism and bile acid synthesis (18–20), dysregulation of iron metabolism was also suspected in *Hnf4a*^{ΔH} mice.

In this study, *Hnf4a*^{ΔH} mice were found to exhibit iron metabolism-related phenotypes, resulting in hypoferrremia, but no iron deficiency anemia and hemochromatosis was observed. Gene expression profiling revealed that hepatic expression of *Tfr2* mRNA was markedly decreased in *Hnf4a*^{ΔH} mice. Promoter analysis showed that the *Tfr2* distal promoter region containing GC-rich sequences was required for basal transactivation of the *Tfr2* gene. In addition, two HNF4 α -binding sites in the proximal promoter region were essential for the maximal transactivation in combination with the proximal GC-rich sequences, revealing that *Tfr2* is a novel HNF4 α target gene in liver.

Experimental Procedures

Animal—Liver-specific *Hnf4a*-null (*Hnf4a*^{ΔH}) mice and liver-specific *Cebpa*-null (*Cebpa*^{ΔH}) mice were described previously (18, 21). All experiments were performed with 45-day-old male *Hnf4a*-floxed (*Hnf4a*^{f/f}) and *Hnf4a*^{ΔH} mice and 2-month-old male *Cebpa*-floxed (*Cebpa*^{f/f}) and *Cebpa*^{ΔH} mice. Mice were housed in a pathogen-free animal facility under standard 12-h light/12-h dark cycle with water and chow *ad libitum*. All experiments with mice were carried out under Association for Assessment and Accreditation of Laboratory Animal Care guidelines with approval of the Animal Care and Use Committee of the NCI, National Institutes of Health, and Gunma University Animal Care and Experimentation Committee.

Serum and Liver Iron Measurements—Mice were anesthetized with 2.5% avertin and decapitated, and trunk blood was collected for the measurement of red blood cells (RBC), hemoglobin, hematocrit, and the mean cell volume, or collected in a serum separator tube (BD Biosciences). The serum was separated by centrifugation at 7,000 × *g* for 5 min and stored at –20 °C prior to analysis. The serum iron concentration and the unsaturated iron-binding capacity were determined colorimetrically using iron and the total iron-binding capacity kit (Sigma). The total iron-binding capacity was calculated by adding the serum iron concentration and the unsaturated iron-binding capacity. Transferrin saturation (%) was calculated as (serum iron concentration/total iron-binding capacity) × 100. Livers were perfused with phosphate-buffered saline (PBS) to remove serum iron, excised, and dried at 100 °C for 16 h. Dried liver samples were dissolved in acidic solution (3 N HCl, 0.6 M trichloroacetic acid) and incubated at 65 °C for 20 h. Extracted iron solution was reacted with chromogen solution (1.25 M acetic acid (pH 4.7), 0.008% bathophenanthroline, 0.08% glyceric acid) at room temperature for 30 min, and the liver iron was determined colorimetrically at 510 nm.

IronChip Analysis—For the cDNA microarray experiments, the “IronChip” (version 3.0) was used. Experimental details concerning the selection of the cDNA clones, the preparation of the microarray platform, the synthesis of fluorescent cDNA probes, prehybridization, and hybridization conditions of the

microarrays as well as scanning and data analysis are described elsewhere (22–24). The symbols of the genes mentioned and RefSeq accession number in the text are summarized in Table 4.

RNA Extraction, Reverse Transcription, and Real Time PCR—Total RNA from the mouse livers and HepG2 cells was extracted using Tripure Isolation Reagent (Roche Applied Science, Tokyo, Japan). cDNA was transcribed using ReverTra Ace qPCR RT Master Mix with gDNA Remover (TOYOBO, Osaka, Japan), and real time PCR was performed using FastStart SYBR Green Master Mix (Roche Applied Science) with the specific primers on LightCycler 480 System II (Roche Applied Science). Levels of mRNA expression were normalized relative to *Gapdh* mRNA as an internal control using the $\Delta\Delta C_t$ method. The following primers were used for real time PCR: mouse *Hnf4a* (agaggttctgtccacagatc and cgctctgtgatggcaatc); human HNF4A (caggctcaagaaatgcttcc and ggctgctgctcctcatagctt); mouse *Tfr2* (ctatctggctctgatcacct and tcagggtg-acatcttcatcga); human TFR2 (gtggaccgacacgcactac and tgtagggcagtagacgctcag); mouse *Gapdh* (gacttcaacagcaactcccac and tcaccaccctgttctgta); human GAPDH (agccacatcgctcagacac and gcccaatcagcaaatcc); mouse *Tf* (cgagctctcttgagaagc and agcctgggacagcttgac); mouse *Hjv* (gccaacgctaccaccatc and tcaaggtcaggaagatt); mouse *Ftl* (ttttgatcgggatgacgtg and cgcttctgaaactcaggagac); mouse *Fth* (tggagttgtatgctcctcag and tggagaaagtattggcaaagtt); mouse *Hpx* (ggaagaatcccatcacctca and caggagggtacaccagact); mouse *Cat* (cctcaagttgtaatgcaga and caagttttgatgcccctgtt); mouse *Sod1* (ccatcagatggggacaataca and ggtctccaacatgcctctct); mouse *Gpx1* (ggtttcccgtgcaatcag and tcggagctacttgagggaat); mouse *Tfr1* (tggaatcccagcagtttctt and gctgctgtacgaaccattt); mouse *Hamp* (gatggcactcagactcg and ctgcagctctgtagtctgtctca); mouse *Hfe* (ggaaaaggaaggtctcagga and cctcaagctctttggctgag); mouse *Fpn1* (tggccactctctcctcactt and tgtaagagaaggctgtttcc); mouse *Heph* (tctatacatgccc-atggattct and tggagtttccactggtaagt); mouse *Cp* (gggcaatgaa-aatatgcaa and tcaaacactgtgggaacaagt); and mouse *Cebpa* (tgg-acaagaacagcaacgag and tcaactgtgtaactccagc).

Cloning of Promoter Region of Mouse *Tfr2* Gene—The –1972, –982, –396, –241, –116, –82, –66, –46/+67, –116, –46, +505/+1144, –46, –116/+504, and –116/+896 fragments from the transcription start site of the mouse *Tfr2* promoter containing KpnI and XhoI sites were amplified with genomic DNA from mouse liver by PCR and cloned into the luciferase reporter vector, pGL4.11 (Promega, Madison, WI). HSV-TK mini and HSV-TK promoters were amplified with pGL4.74 (Promega) by PCR and cloned into EcoRV and BglII/HindIII sites of the pGL4.11 and named pGL4.11/TK and pGL4.11/TK mini, respectively. Mutations were introduced into GC-rich sequences and HNF4 α -binding sites in the *Tfr2* promoter by overlapped or inverted PCR-based site-directed mutagenesis. The following primers were used for amplification of HSV-TK mini promoter (ggcatagatctttcgatattaaggtgacgcgtgtggcctc and ggcaataagcttttaagcgggtcgcgtgcagggtcgcctcggtg) and the TK promoter (gcataagcttaaatgagctcttcggacactcg and ggcaataagcttttaagcgggtcgcgtgcagggtcgcctcggtg). Similarly, the following primers were also used for PCR-based mutagenesis of GC-1 region (attgtttagctcctctggggcgg and aacaatcgcacgtcctttct), GC-2 region (tttacattgctggggcgtgctct and caaatgtaaaagaggactccgcc), GC-3 region (taactaactctagtggtgtgg and ttagttacaggc-

ccccccag), the HNF4 α -binding site at +182/+201 (**tgacgct-gtga**ttccattcacagctgc and acctcacccttactctggtccagg), and the distal HNF4 α -binding site at +830/+842 (**cgcgctgctgctgaggtt**-taaaaa and ggccaacttggtccctcacaggt). The induced mutations are indicated as bold and underlined.

Transient Transfection and Luciferase Assays—HepG2 and HEK293T cells were cultured at 37 °C in Dulbecco's modified Eagle's medium (WAKO, Osaka, Japan) containing 10% fetal bovine serum (HyClone, Logan, UT) and 100 units/ml penicillin/streptomycin (Invitrogen). For suspension transfection, wild type or mutated *Tfr2* promoters cloned into pGL4.11 and pGL4.74 encoding *Renilla* luciferase regulated by the HSV-TK promoter as an internal control were transfected into HepG2 cells with polyethyleneimine max (Polyscience, Warrington, PA) as a transfection reagent. For co-transfection using HEK293T cells, HNF4 α expression plasmid, pSG5/HNF4 α , was used (19). After 48 h, the cells were washed with phosphate-buffered saline (PBS), and promoter activities were measured using Dual-Glo Luciferase Assay System (Promega).

Transfection of siRNA—Two kinds of siRNA for human HNF4 α (10 nM, Sigma, Tokyo, Japan) were independently transfected into HepG2 cells with Lipofectamine RNAiMAX (Life Technologies, Inc.). After 48 h, cells were trypsinized and re-transfected with 10 nM of the same siRNA. After 48 h of re-transfection, cells were harvested, and total RNA was extracted using Tripure Isolation Reagent for RT quantitative PCR. Nucleotide sequences for the siRNA duplexes targeting human HNF4 α are follows: GGCAGUGCGUGGUGGACAA for siHNF4 α -1 and AGAGAUCCAUGGUGUCAA for siHNF4 α -2.

Western Blot—Liver samples from *Hnf4a*^{f/f} and *Hnf4a*^{ΔH} mice were homogenized in lysis buffer (7 M urea, 2 M thiourea, 1% Triton X-100) and allowed to sit on ice for 30 min. The homogenate was centrifuged at 12,000 × *g* for 30 min at 4 °C, and the supernatants were used as whole cell lysates. The whole cell lysates and serum protein (40 μg), determined by Quick StartTM Bradford Dye Reagent (Bio-Rad), were diluted with Laemmli sample buffer, incubated at 65 °C for 15 min, and fractionated by 10% SDS-PAGE. The gels were stained with Coomassie Brilliant Blue R-250 or transferred onto a PVDF membrane (GE Healthcare, Tokyo, Japan). The membrane was incubated for 1 h with PBS containing 0.1% Tween 20 and 5% skim milk and then incubated for 1 h with anti-transferrin (Santa Cruz Biotechnology, Dallas, TX), anti-transferrin receptor 2 (Abcam, Tokyo, Japan), and anti- γ -tubulin (TUBG) (Sigma) antibodies. After washing, the membrane was incubated for 1 h with horseradish peroxidase-conjugated secondary antibodies (Santa Cruz Biotechnology), and the reaction product was visualized using SuperSignal West Pico Chemiluminescent Substrate (Pierce). Expression of TF and TFR2 proteins was quantified by densitometric analysis using ImageJ software and the expression in *Hnf4a*^{ΔH} was presented as expression differences relative to the *Hnf4a*^{f/f} mice.

Gel Mobility Shift Analysis—Nuclear extracts from HepG2 cells were prepared using NE-PER nuclear and cytoplasmic extraction reagents (Thermo Fisher Scientific, Yokohama, Japan), and gel shift analysis was carried out using LightShift Chemiluminescent EMSA kit (Thermo Fisher Scientific). The

following double-stranded probes were used (mutations are indicated as bold and underlined); the HNF4 α -binding site at +182/+201 in the mouse *Tfr2* promoter (wild type, gggtaggtggacacctgaacttccattcacagctgca and **tgacgctg**tgatgggaaagtcca-gggtccacctcacc; mutant, gggtaggt**tgacgctg**tgat**ttccattcacagctgca** and **tgacgctg**tgatgggaaat**tcacagcgtca**acctcacc); the HNF4 α -binding site at +830/+842 in the mouse *Tfr2* promoter (wild type, gaaccaagttggccaaagtctgctctgaggt and acctcagagcagactttggccaacttggttc; mutant, gaaccaagttggcc**cgcgctgctgctgaggt** and acctcagagcagac**cggggccaacttggttc**); and the HNF4 α -binding site at -203/-192 in the mouse ornithine transcarbamylase (*Otc*) promoter as a positive control (gttaggcttaaagttcagtg and cacttgaactttaagcctaac) (19). Nuclear extracts (3 μg) and the 5'-biotin-labeled probes of the HNF4 α -binding sites for the *Tfr2* promoter (wild type) were added, and the reaction mixture was incubated on ice for 10 min. For competition experiments, a 50-fold excess of unlabeled probe was added to the reaction mixture, and the mixture was incubated on ice for 10 min prior to the addition of the 5'-biotin-labeled probe. For supershift analysis, 1 μg of anti-HNF4 α or anti-peroxisome proliferator-activated receptor α antibodies (Santa Cruz Biotechnology) was added to the reaction mixture, and the mixture was incubated on ice for 10 min after the addition of the 5'-biotin-labeled probe. DNA-protein complexes were fractionated by 7% PAGE containing 5% glycerol and blotted onto a Biotinylated nylon membrane (Pall, Tokyo, Japan). After washing, DNA-protein complexes were visualized using a detection module in the kit on an ImageQuant LAS4000.

Chromatin Immunoprecipitation—HepG2 cells cultured in a 10-cm dish were fixed in 0.5% formaldehyde for 10 min and then quenched with 125 mM glycine for 5 min at room temperature. After washing with ice-cold PBS, the cells were resuspended in 3 ml of Lysis buffer 1 (50 mM HEPES-KOH (pH 7.5), 140 mM NaCl, 1 mM EDTA, 10% glycerol, 0.5% Nonidet P-40, 0.25% Triton X-100, and protease inhibitor (Roche Applied Science)) on ice for 10 min and then centrifuged at 1,400 × *g* for 5 min. The cell pellet was resuspended in 3 ml of Lysis buffer 2 (10 mM Tris-HCl (pH 8.0), 200 mM NaCl, 1 mM EDTA, and 5 mM EGTA) for 10 min at room temperature and then centrifuged at 1,400 × *g* for 5 min. The cell pellet was resuspended in 1 ml of Lysis buffer 3 (10 mM Tris-HCl (pH 8.0), 300 mM NaCl, 1 mM EDTA, 0.5 mM EGTA, and 0.1% sodium deoxycholate). Liver samples stored at -80 °C were ground to pieces with a pestle and mortar under liquid nitrogen and fixed in PBS containing 20 mM sodium butyrate, 1% formaldehyde, and protease inhibitor mixture for 10 min at room temperature. After centrifugation, the pellet was resuspended in Lysis buffer (50 mM Tris-HCl (pH 8.0), 10 mM EDTA, 1% SDS, and 20 mM sodium butyrate). The cell lysate from HepG2 cells and liver samples was disrupted by an ultrasonicator (UR-20P, TOMY, Tokyo, Japan) for 5 min on ice and then 1% Triton X-100 was added, followed by centrifuging at 20,000 × *g* for 10 min. A small volume of the supernatant was stored at 4 °C as the input samples. The remaining supernatant was pre-cleared by adding of 15 μl of a 50% slurry of protein G-Sepharose 4 Fast Flow (GE Healthcare) with sonicated salmon sperm DNA and rotated for 4 h at 4 °C, followed by centrifuging at 1,900 × *g* for 5 min. The supernatant was divided into two pieces and incubated with anti-

Regulation of *Tfr2* by Hepatic HNF4 α

TABLE 1

Serum iron content in *Hnf4a*^{ΔH} mice

Values are presented as mean ± S.D. (*n* = 8). TIBC is total iron-binding capacity. Significant differences are compared with *Hnf4a*^{f/f} mice.

Mice	Iron	TIBC	Transferrin saturation
<i>Hnf4a</i> ^{f/f}	μg/dl 235.7 ± 43.1	μg/dl 751.8 ± 223.1	% 34.6 ± 15.3
<i>Hnf4a</i> ^{ΔH}	95.7 ± 22.8 ^a	336.9 ± 150.9 ^a	34.8 ± 19.8

^a *p* < 0.005.

HNF4 α antibody (4 μg, Santa Cruz Biotechnology) or control normal goat IgG for 16 h at 4 °C. The reaction mixture was centrifuged at 1,900 × *g* for 5 min at 4 °C, and the pellet collected was washed for 5 min at 4 °C with 1 ml of RIPA-1 buffer (50 mM Tris-HCl (pH 8.0), 150 mM NaCl, 1 mM EDTA, 1% Triton X-100, 0.1% SDS, and 0.1% sodium deoxycholate), RIPA-2 buffer (50 mM Tris-HCl (pH 8.0), 300 mM NaCl, 1 mM EDTA, 1% Triton X-100, 0.1% SDS, and 0.1% sodium deoxycholate), LiCl wash solution (10 mM Tris-HCl (pH 8.0), 0.25 M LiCl, 1 mM EDTA, 0.5% Nonidet P-40, and 0.5% sodium deoxycholate), and TE (10 mM Tris-HCl (pH 8.0) and 1 mM EDTA), respectively. Then the ChIP direct elution buffer (10 mM Tris-HCl (pH 8.0), 300 mM NaCl, 5 mM EDTA, and 0.5% SDS) was added to the pellet and incubated for 16 h at 65 °C for decross-linking. After treatment with RNase A for 30 min at 37 °C and proteinase K for 2 h at 55 °C, the DNA was purified and used for PCR and real time PCR. Enrichment of the HNF4 α binding was normalized to the input samples using the $\Delta\Delta C_t$ method and expressed as fold-enrichment as compared with the control normal IgG antibody. The following primers were used for amplification of the HNF4 α -binding sites in the human *TFR2* promoter (gggaactaggaggccaaagt and tctcccctgccaatctctc), the human *MIR-194/192* gene without HNF4 α -binding site as a negative control (cctgtgagggcacacctt and aaagccaggcagtcagt-gct), the HNF4 α -binding sites in the mouse *Tfr2* promoter (caggaagaccggtaacg and tcttggtctggtgctagg), and the mouse *Hmgcs2* gene without HNF4 α -binding site as a negative control (gatccctgggactcacaca and gaatgcacattatggaggctca).

Statistical Analysis—All values are expressed as the mean ± S.D. All data were analyzed by the unpaired Student's *t* test for significant differences between the mean values of each group.

Results

***Hnf4a*^{ΔH} Mice Exhibit Hypoferremia**—Hematological parameters are good indicators for alternation of iron homeostasis. Here, hepatic HNF4 α was found to maintain serum iron levels (Table 1). *Hnf4a*^{ΔH} mice exhibited a 60% reduction in serum iron compared with control *Hnf4a*^{f/f} mice. Likewise, total iron binding capacity, an index of the total amount of serum iron that transferrin can bind, was also reduced in *Hnf4a*^{ΔH} mice, indicating a lower availability of transferrin protein in *Hnf4a*^{ΔH} mice. However, because no significant difference in transferrin saturation was observed in *Hnf4a*^{ΔH} mice, iron-binding transferrin is normal in *Hnf4a*^{ΔH} mice. Moreover, red blood cell counts (RBC), hemoglobin levels, the hematocrit, and the mean cell volume were unchanged in *Hnf4a*^{ΔH} mice compared with *Hnf4a*^{f/f} mice (Table 2). Furthermore, no significant difference in liver iron content was detected in *Hnf4a*^{ΔH} mice (Table 3), suggesting that *Hnf4a*^{ΔH} mice do

TABLE 2

Hematological parameters in *Hnf4a*^{ΔH} mice

RBC is red blood cells; HGB is hemoglobin; MCV is mean corpuscular volume; HCT is hematocrit. All values are presented as means ± S.D. (*n* = 3–5).

Mice	RBC	HGB	MCV	HCT
<i>Hnf4a</i> ^{f/f}	M/μl 9.2 ± 0.1	g/dl 14.3 ± 0.1	fl 49.6 ± 2.0	% 45.7 ± 1.5
<i>Hnf4a</i> ^{ΔH}	10.2 ± 0.2	14.8 ± 1.3	47.6 ± 2.8	49.1 ± 3.6

TABLE 3

Liver iron content in *Hnf4a*^{ΔH} mice

Values are presented as mean ± S.D. (*n* = 5).

Mice	Iron
<i>Hnf4a</i> ^{f/f}	μg/g liver 235 ± 92
<i>Hnf4a</i> ^{ΔH}	200 ± 108

not develop liver iron deficiency disease nor hereditary hemochromatosis.

Expression of Genes Involved in Iron Metabolism is Altered in *Hnf4a*^{ΔH} Mice—The expression profile of mRNAs encoded by iron metabolism-related genes was analyzed in *Hnf4a*^{ΔH} and *Hnf4a*^{f/f} mouse livers using IronChip microarray analysis (Table 4). Hepatic expression of many mRNAs significantly changed in *Hnf4a*^{ΔH} mice. Among the down-regulated mRNAs were transferrin (*Tf*), transferrin receptor 2 (*Tfr2*), hemojuvelin (*Hjuv*), ferritin light chain (*Ftl*), ferritin heavy chain (*Fth*), hemopexin (*Hpx*), catalase (*Cat*), Cu-Zn superoxide dismutase (*Sod1*), and glutathione peroxidase 1 (*Gpx1*). Up-regulated mRNAs included transferrin receptor 1 (*Tfr1*), hepcidin (*Hamp*), and ceruloplasmin (*Cp*) mRNAs. Microarray data were validated by quantitative RT-PCR (Fig. 1A). Because atransferrinemia/hypotransferrinemia is caused by recessive mutations in the *Tf* gene resulting in iron-deficient hypochromic anemia in humans and mice (25, 26), reduced expression of TF may cause hypoferremia. Indeed, as expected from reduced *Tf* mRNA expression, serum TF protein in *Hnf4a*^{ΔH} mice was decreased by 66% compared with *Hnf4a*^{f/f} mice (Fig. 1B). These data show that misregulation of a previously validated HNF4 α target gene is preserved in *Hnf4a*^{ΔH} mice (15). Thus, HNF4 α -dependent regulation of *Tf* could partially contribute to the hypoferremia observed in this mouse model.

In addition, decreased expression of hepatic *Tfr2* mRNA to 30% was observed in *Hnf4a*^{ΔH} mice, although expression of *Tfr1* mRNA encoding a receptor with affinity to holo-TF 25-fold higher than TFR2 was increased to 4-fold (Fig. 1A) (8). TFR2 protein in *Hnf4a*^{ΔH} mice was also decreased by 19% compared with *Hnf4a*^{f/f} mice (Fig. 1C). Because TFR2 and HNF4 α are highly expressed in the liver and mutations in the *TFR2* gene cause type III hemochromatosis in humans (6, 7), further studies were focused on the *Tfr2* gene. Previous reports suggest that the promoter activity of the *Tfr2* gene was induced by C/EBP α expression (27). However, expression of hepatic *Tfr2* was unchanged in liver-specific *Cebpa*-null (*Cebpa*^{ΔH}) mice (Fig. 1D), indicating that C/EBP α is unlikely to be the main regulator of *Tfr2* expression in the liver.

Promoter Analysis of the Distal Region of the *Tfr2* Promoter—Promoter analysis of the mouse *Tfr2* gene was performed to determine whether HNF4 α directly regulates *Tfr2* expression.

TABLE 4

Expression profiling of hepatic mRNA involved in iron metabolism in *Hnf4a*^{ΔH} mice

Microarray analysis was performed using pooled total RNA from liver tissues of *Hnf4a*^{ΔH} and *Hnf4a*^{f/f} mice. Ratio of expression levels between both of them was indicated as fold-change.

Gene symbol	Ref. Seq. (NM_)	Fold-change (<i>Hnf4a</i> ^{ΔH} / <i>Hnf4a</i> ^{f/f})	Gene symbol	Ref. Seq. (NM_)	Fold-change (<i>Hnf4a</i> ^{ΔH} / <i>Hnf4a</i> ^{f/f})
<i>Tf</i>	133977	0.17	<i>Irp1</i>	007386	0.72
<i>Ltf</i>	008522	0.19	<i>Fth</i>	010239	0.73
<i>Mgst1</i>	019946	0.29	<i>Zfp36</i>	011756	0.82
<i>Tfr2</i>	015799	0.30	<i>Fmo2</i>	018881	1.31
<i>Atp7b</i>	007511	0.33	<i>Npm1</i>	008722	1.38
<i>Selp</i>	011347	0.33	<i>Hif1a</i>	010431	1.39
<i>Cat</i>	009804	0.38	<i>Fmo1</i>	010231	1.42
<i>Efna1</i>	010107	0.44	<i>Mt3</i>	013603	1.47
<i>Gpx1</i>	008160	0.48	<i>Srsf3</i>	013663	1.52
<i>Sod1</i>	011434	0.48	<i>Por</i>	008898	1.53
<i>Ldh1</i>	010699	0.50	<i>Cox17</i>	001017429	1.55
<i>Rplp0</i>	007475	0.51	<i>Arg1</i>	007482	1.58
<i>Atp7a</i>	009726	0.52	<i>Maob</i>	172778	1.61
<i>Prodh</i>	011172	0.53	<i>Hamp</i>	032541	1.68
<i>Nr1i3</i>	009803	0.56	<i>Hspa8</i>	031165	1.71
<i>Fil</i>	010240	0.58	<i>Cp</i>	007752	1.72
<i>Acss2</i>	019811	0.58	<i>Hspa5</i>	022310	1.72
<i>Slc31a1</i>	175090	0.60	<i>Psap</i>	011179	1.72
<i>Hpx</i>	017371	0.63	<i>App</i>	007471	1.88
<i>Acox3</i>	030721	0.63	<i>Gsn</i>	146120	1.89
<i>Atox1</i>	009720	0.64	<i>Tfr1</i>	011638	3.31
<i>Impa1</i>	018864	0.64	<i>Mt1</i>	013602	3.80
<i>Cyp3a13</i>	007819	0.64	<i>Fmo3</i>	008030	4.34
<i>Cyp1a1</i>	009992	0.65	<i>Spp1</i>	009263	5.05
<i>Txn1</i>	011660	0.70	<i>Mt2</i>	008630	6.19
<i>Nfs1</i>	010911	0.70			

Analysis of the distal promoter was carried out in HepG2 cells that highly express endogenous HNF4 α and TFR2 (6) revealing significant promoter activities with the region between -116 and -46 from the transcription start site (Fig. 2B). Activity of the *Otc* promoter that has two HNF4 α -binding sites was completely suppressed by HNF4 α knockdown using siRNA; however, no repression of the promoter activities was detected in all *Tfr2* promoters by siRNA against HNF4 α (Fig. 2C), indicating that the distal promoter of the *Tfr2* gene was activated in an HNF4 α -independent manner. Searching the JASPER database for transcription factor-binding sites in the region between -116 and -46 revealed three GC boxes (GC-1, 2, and -3) that were predicted between -91 and -53 (Fig. 2D). Furthermore, the stepwise transactivation of the promoter activity was observed in the presence of these GC boxes (Fig. 2B). To determine which regions of these GC boxes are sufficient for transactivation, mutations were introduced into each GC box. Mutations of the GC-2 region significantly suppressed the promoter activity, and mutations of all GC regions further suppressed the activity (Fig. 2E), indicating that the GC-2 region is a central *cis*-element for transactivation, and the GC-1 and GC-3 regions are required for the maximal transactivation of the distal promoter.

Promoter Analysis of the Proximal Region of the *Tfr2* Promoter—As described above, regions that respond to HNF4 α were not identified in the distal promoter. No transactivation was detected in this promoter region ($+505/+1144$ and $-46/+1144$) as compared with the promoterless and the distal promoter ($-116/+67$, see Fig. 3A). Therefore, the proximal promoter was analyzed for the presence of an HNF4 α -dependent enhancer. At first, the full-length proximal promoter ($-46/+1144$) had enhancer activity in the presence of the core *Tk* promoter (Fig. 3B). In addition, the shorter promoter regions ($-46/+505$ and $-46/+1144$) had weak enhancer activities,

showing that these regions might cooperatively contribute to enhancer transactivation. Next, the $-46/+504$ and $+505/+1144$ proximal promoters were transactivated by HNF4 α expression vector, and the full-length promoter was further transactivated by HNF4 α in the presence of the *Tk* mini promoter (Fig. 3C). These results indicate that the proximal promoter contains at least two HNF4 α -dependent elements located at $-46/+504$ and $+505/+1144$. In addition, the proximal promoters with the distal promoter ($-116/+504$, $-116/+896$, and $-116/+1144$) was also transactivated by HNF4 α as compared with the distal promoter alone ($-116/+67$), with the result that HNF4 α has the potential to transactivate the native *Tfr2* promoter via two regions located at $+67/+504$ and $+505/+896$ (Fig. 3D). By searching with the JASPER database, three potential HNF4 α -binding sites were found at $+182/+194$, $+189/+201$, and $+830/+842$, and the binding sites located at $+182/+194$ and $+189/+201$ overlapped (Fig. 3E). Of these, the binding site at $+830/+842$ was highly conserved among species (Fig. 4A). To determine whether these predicted HNF4 α -binding sites could transactivate the *Tfr2* gene in an HNF4 α -dependent manner, mutations were introduced into the binding sites. Because the binding site at $+182/+194$ and $+189/+201$ overlapped, mutations were introduced into the middle region at $+182/+201$ so that HNF4 α could not bind to both sites. Consequently, disruption of each binding site decreased HNF4 α -dependent transactivation, and disruption of both binding sites further repressed the transactivation, indicating that these HNF4 α -binding sites were transactivated in an HNF4 α -dependent manner (Fig. 4B).

To investigate whether the minimal promoter region in the distal promoter would be essential for transactivation by HNF4 α , mutations were introduced into both the GC boxes and HNF4 α -binding sites (Fig. 4C). In the presence of the HNF4 α -binding sites in the proximal promoter, mutations of

Regulation of *Tfr2* by Hepatic HNF4 α

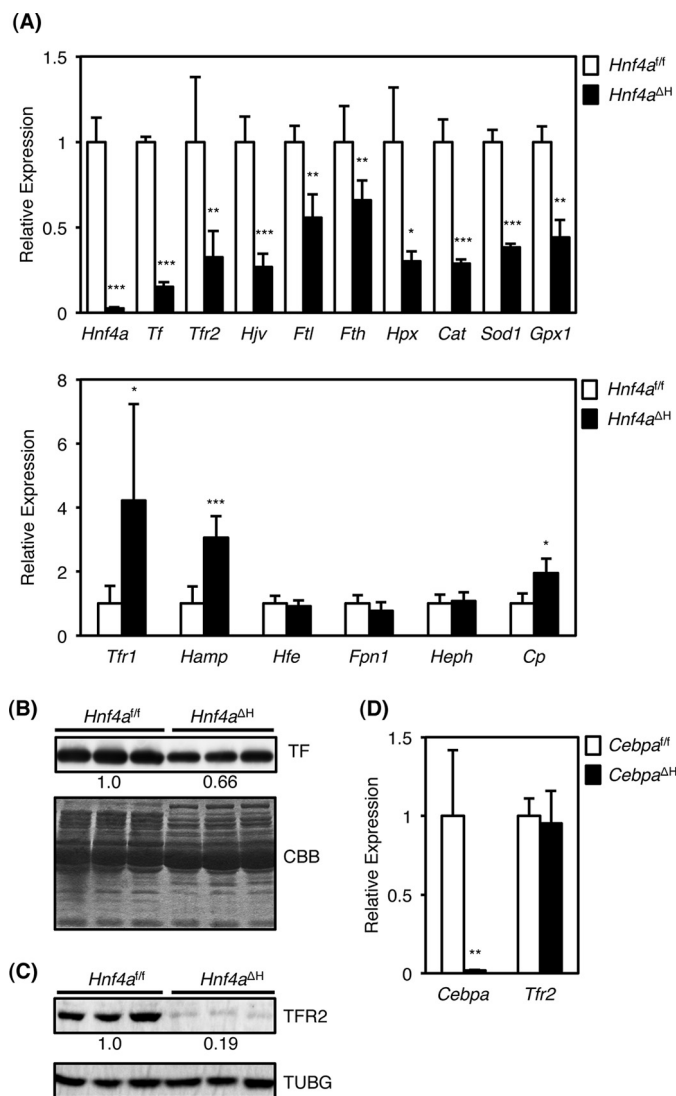


FIGURE 1. Hepatic expression of iron metabolism-related genes in *Hnf4a* Δ^H mice. A, real time PCR for *Hnf4a*, *Tf*, *Tfr2*, *Hjv*, *Ftl*, *Fth*, *Hpx*, *Cat*, *Sod1*, and *Gpx1* (upper panel), and *Tfr1*, *Hamp*, *Hfe*, *Fpn1*, *Heph*, and *Cp* (lower panel) mRNAs from total liver RNA of *Hnf4a* Δ^H and *Hnf4a* $^{fl/fl}$ mice ($n = 5$ for each genotype). The normalized expression in *Hnf4a* Δ^H mice was presented relative to that in *Hnf4a* $^{fl/fl}$ mice. B, Western blot of TF protein from serum of *Hnf4a* Δ^H and *Hnf4a* $^{fl/fl}$ mice ($n = 3$ for each genotype) (upper panel). Coomassie Brilliant Blue stain of serum total protein of *Hnf4a* Δ^H and *Hnf4a* $^{fl/fl}$ mice as loading controls (lower panel). The expression of TF protein was quantified by densitometric analysis using ImageJ software. The normalized TF expression in *Hnf4a* Δ^H was presented as relative to that in *Hnf4a* $^{fl/fl}$ mice. C, Western blot of TFR2 (upper panel) and TUBG (lower panel) protein from livers of *Hnf4a* Δ^H and *Hnf4a* $^{fl/fl}$ mice ($n = 3$ for each genotype). The TFR2 expression normalized by TUBG in *Hnf4a* Δ^H was presented as relative to *Hnf4a* $^{fl/fl}$ mice. D, real time PCR for *Cebpa* and *Tfr2* mRNAs from total liver RNA of *Cebpa* Δ^H and *Cebpa* $^{fl/fl}$ mice ($n = 5$ for each genotype). The normalized expression in *Cebpa* Δ^H mice was presented relative to that in *Cebpa* $^{fl/fl}$ mice. Data are mean \pm S.D. *, $p < 0.05$; **, $p < 0.01$; ***, $p < 0.001$.

the GC-2 region (GC2/M) inhibited the transactivation by HNF4 α by about 35% as compared with the wild-type promoter (−116/+1144WT). Mutations of each HNF4 α -binding site with mutations of the GC-2 region (GC2/M-H4/M1 and GC2/M-H4/M2) markedly suppressed the transactivation by HNF4 α , and further suppression was detected by mutations in both HNF4 α -binding sites (GC2/M-H4/M1+M2). Additionally, mutations of all GC boxes (GC-all/M) further inhibited the

transactivation by HNF4 α when compared with that of the mutations of the GC-2 region alone (GC2/M). Transactivation by HNF4 α was particularly inhibited by mutations in all GC regions and HNF4 α -binding sites, indicating that the GC-2 region plays a critical role in transactivation of the *Tfr2* gene by HNF4 α .

Direct Binding of HNF4 α to the Proximal Region of the *Tfr2* Promoter—To determine whether HNF4 α can directly bind to both HNF4 α -binding sites in the *Tfr2* promoter, gel mobility shift analysis was performed (Fig. 5A). Nuclear extracts from HepG2 cells bound to the distal (+182/+201) and proximal (+830/+842) HNF4 α -binding sites (Fig. 5A, lane 2, lower arrows). This complex was diminished by the addition of excess amounts of unlabeled *Tfr2* competitor and the *Otc* competitor that contains a *bona fide* HNF4 α -binding site (Fig. 5A, lanes 3 and 4) (19) but not the competitor that has mutations in the HNF4 α -binding site of the *Tfr2* promoter (Fig. 5A, lane 5). Moreover, the complex was supershifted by anti-HNF4 α antibody (Fig. 5A, lane 6, upper arrow) but not the unrelated anti-peroxisome proliferator-activated receptor α antibody (lane 7). These results indicate that HNF4 α indeed binds to the distal and proximal regions of the *Tfr2* promoter. Next, chromatin immunoprecipitation (ChIP) was used to determine whether HNF4 α directly binds to the *Tfr2* promoter *in vivo*. HNF4 α bound to the predicted HNF4 α -binding sites in HepG2 cells as compared with IgG control (Fig. 5B). In addition, ChIP analysis using the livers of *Hnf4a* $^{fl/fl}$ and *Hnf4a* Δ^H mice indicated that hepatic HNF4 α in *Hnf4a* $^{fl/fl}$ mice significantly bound to the promoter region, and the binding was lower in *Hnf4a* Δ^H mouse livers (Fig. 5C), suggesting that HNF4 α directly and physiologically binds to the promoter region of the *Tfr2* gene in human and mouse liver.

To determine whether regulation of hepatic *Tfr2* expression by HNF4 α observed in mice could be also maintained in a human hepatocyte-derived cell line, HNF4 α knockdown by siRNAs was performed revealing that HNF4 α was suppressed in HepG2 cells (Fig. 5D). Expression of *TFR2* mRNA was decreased by HNF4 α knockdown, indicating that expression of the *TFR2* mRNA is positively correlated with HNF4 α expression in HepG2 cells (Fig. 5D).

Discussion

The present data show that serum iron levels are decreased in *Hnf4a* Δ^H mice without significant changes in RBC, HBG, and hematocrit and no evidence for iron deficiency anemia. Changes in the expression of multiple genes in *Hnf4a* Δ^H mice make it difficult to ascribe a phenotype to loss of expression of a single gene. However, expression of hepatic *Tf* mRNA and serum TF protein was decreased in *Hnf4a* Δ^H mice, due to loss of direct transactivation of *Tf* by HNF4 α (15). Hypotransferrinemic mice carrying a mutation in the *Tf* gene die from iron deficiency anemia before weaning, but these mice can be rescued by injection of serum or purified TF (26). Thus, the reduced expression of TF would only partially cause hypoferrinemia in *Hnf4a* Δ^H mice. Serum TF protein still remains about 70% of normal as revealed by Western blot data, suggesting that the symptoms in *Hnf4a* Δ^H mice would not be severe enough to develop iron deficiency anemia. Because serum TF protein has

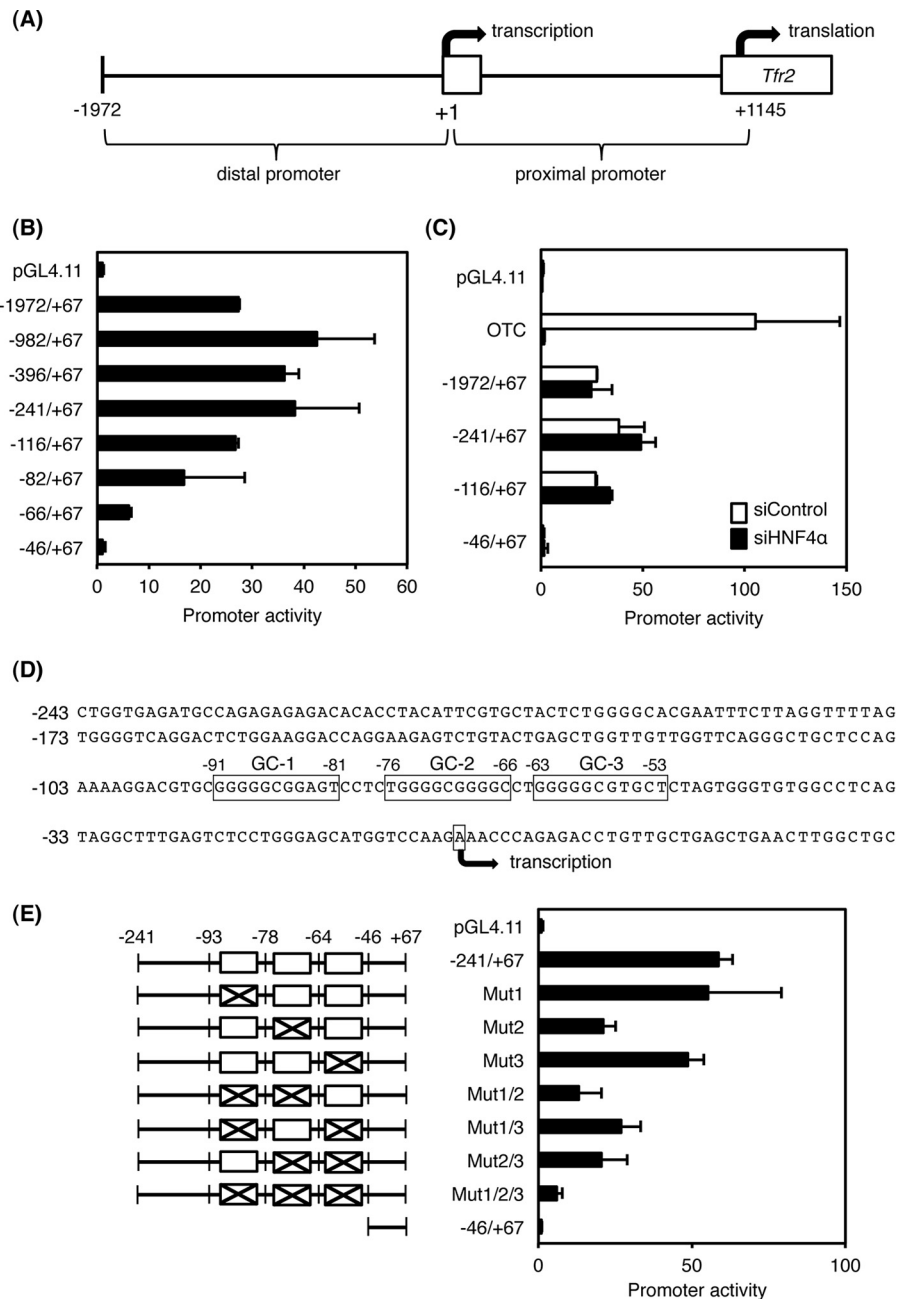


FIGURE 2. Promoter analysis of distal region of the mouse *Tfr2* gene. *A*, schematic structure of the promoter region of the mouse *Tfr2* gene. *B*, promoter activity of the distal region of the *Tfr2* gene in HepG2 cells. *C*, promoter constructs were transfected into HepG2 cells with 20 nM siRNA for HNF4 α (*siHNF4 α*) or negative control (*siControl*). *Otc* promoter whose transactivation is dependent on HNF4 α expression was used as a positive control. *D*, nucleotide sequences of the distal promoter of the *Tfr2* gene. Three GC-rich sequences (GC-1, -2, and -3) are boxed. *E*, mutations were introduced into three GC-rich sequences (1–3) between –93 and –46 in the –241/+67 promoter (*left panel*). The promoter activities were measured in HepG2 cells (*right panel*). The normalized activity \pm S.D. ($n = 3$) was presented as promoter activity based on pGL4.11.

a relatively long half-life (8–10 days), the majority of serum TF protein may remain in *Hnf4a*^{ΔH} mice despite that TF protein is mainly expressed in the liver, and hepatic expression of *Tf* mRNA in *Hnf4a*^{ΔH} mice was decreased to 20% compared with control mice. Furthermore, expression of *Tfr1* mRNA was markedly increased in *Hnf4a*^{ΔH} mice. *Tfr1* mRNA is post-transcriptionally regulated via iron-response elements in the 3'-untranslated regions by iron-regulatory proteins during low iron levels, resulting in *Tfr1* mRNA stabilization and increased TFR1 protein (3, 28). However, both liver iron content and expression of IRP-1 and -2 remained unchanged in *Hnf4a*^{ΔH}

mice, suggesting that TFR1 protein expression would also be increased in *Hnf4a*^{ΔH} mice as well as *Tfr1* mRNA without post-transcriptional regulation. Thus, increased iron uptake into the liver by increased TFR1 may cause the hypoferremia found in *Hnf4a*^{ΔH} mice.

The other cause of hypoferremia in *Hnf4a*^{ΔH} mice might be due to up-regulation of *Hamp* expression. Excess HAMP degrades or internalizes duodenal FPN1 and inhibits iron export into the bloodstream, leading to induction of hypoferremia, and thus the HAMP-FPN1 axis is the most important regulator of iron homeostasis (1, 12). Expression of *HAMP* is

Regulation of *Tfr2* by Hepatic HNF4 α

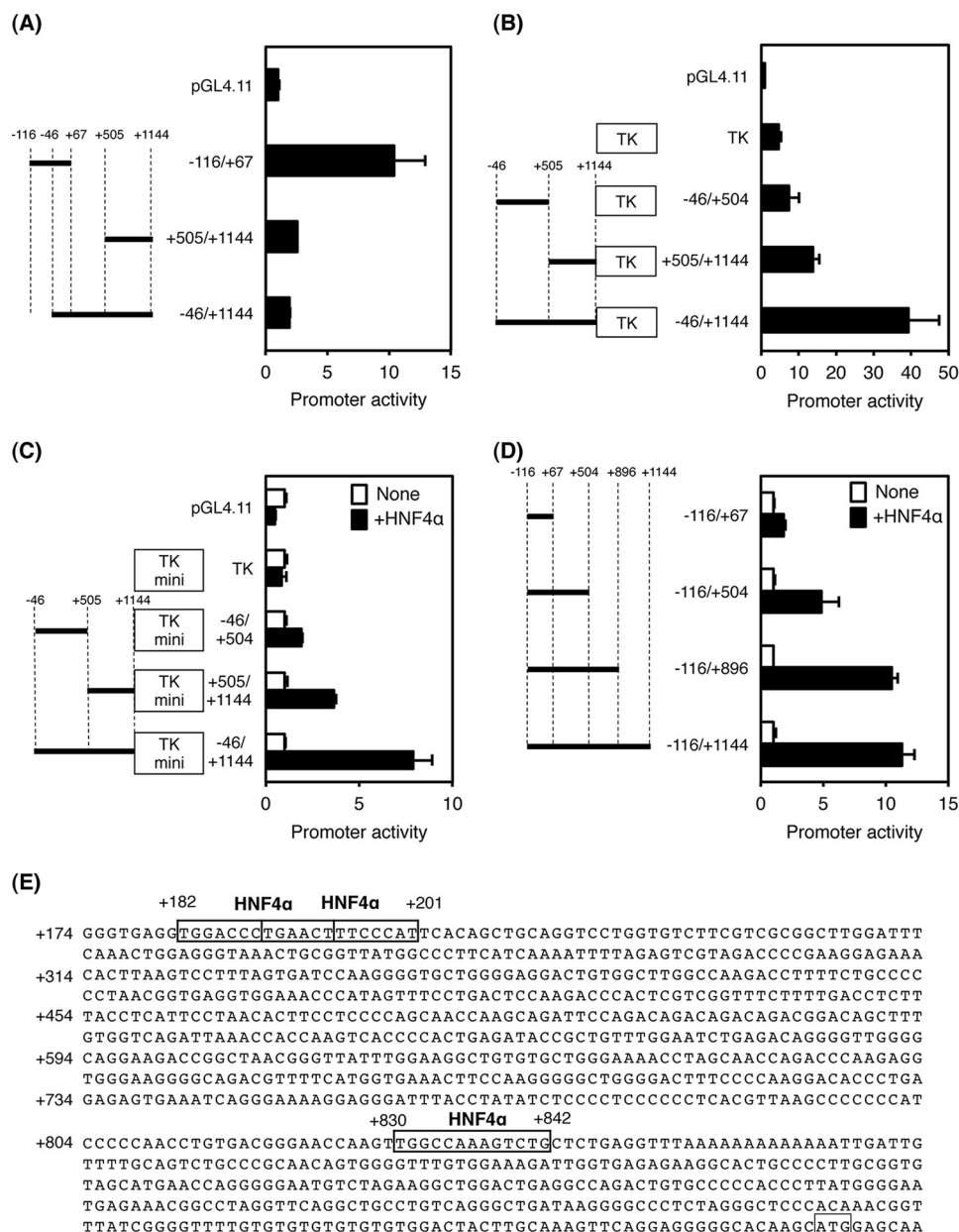


FIGURE 3. Promoter and enhancer analysis of the proximal region of the mouse *Tfr2* gene. *A*, promoter activity of the proximal region of the *Tfr2* gene in HepG2 cells. *B*, enhancer activity of the proximal region of the *Tfr2* gene with TK promoter. *C*, enhancer activity of the proximal region of the *Tfr2* gene with TK mini promoter in HEK293T cells. Empty vector (None), or HNF4 α expression vector (+HNF4 α) was co-transfected. *D*, enhancer activity of the proximal region of the *Tfr2* gene with the distal promoter in HEK293T cells. Empty vector or HNF4 α expression vector was also co-transfected. *E*, nucleotide sequences of the proximal promoter of the *Tfr2* gene. Predicted HNF4 α -binding sites are boxed. The normalized activity \pm S.D. ($n = 3$) is presented as promoter activity based on pGL4.11 (*A* and *B*) or empty vector-transfected control (*C* and *D*).

positively regulated at the transcriptional level through hemoujevin, TFR2, and the pro-inflammatory IL6/STAT3 pathway (1, 2, 10, 29). However, despite the decreased expression of *Hjv* and *Tfr2* mRNA, *Hamp* mRNA is elevated 3-fold in *Hnf4a*^{AH} mice. In contrast, *Hnf4a*^{AH} mice showed hepatosteatosis and increased serum alanine transaminase, an indicator of liver dysfunction and inflammation (18). Moreover, ROS are known to induce inflammation through the production of proinflammatory cytokines (30), and hepatic expression of CAT, SOD1, and GPX1 that degrade ROS was decreased in *Hnf4a*^{AH} mice (31). These data indicate that the accumulation of ROS could lead to liver inflammation, and the resultant up-regulation of *Hamp* in

Hnf4a^{AH} mice could be caused by enhanced inflammatory signaling.

Even though reduced expression of hepatic *Tfr2* that causes hereditary hemochromatosis when mutated in humans (7), *Hnf4a*^{AH} mice did not show evidence of this disorder. Because hepatic *Hamp* expression in both the complete and liver-specific *Tfr2*-null mice was decreased at a similar age as the *Hnf4a*^{AH} mice used in this study (32, 33) and because HAMP is the downstream regulator of TFR2, up-regulation of *Hamp* might be the main reason why *Hnf4a*^{AH} mice do not show hemochromatosis despite the down-regulation of *Tfr2* expression. It is noteworthy that liver-specific *Tfr2*-null mice also

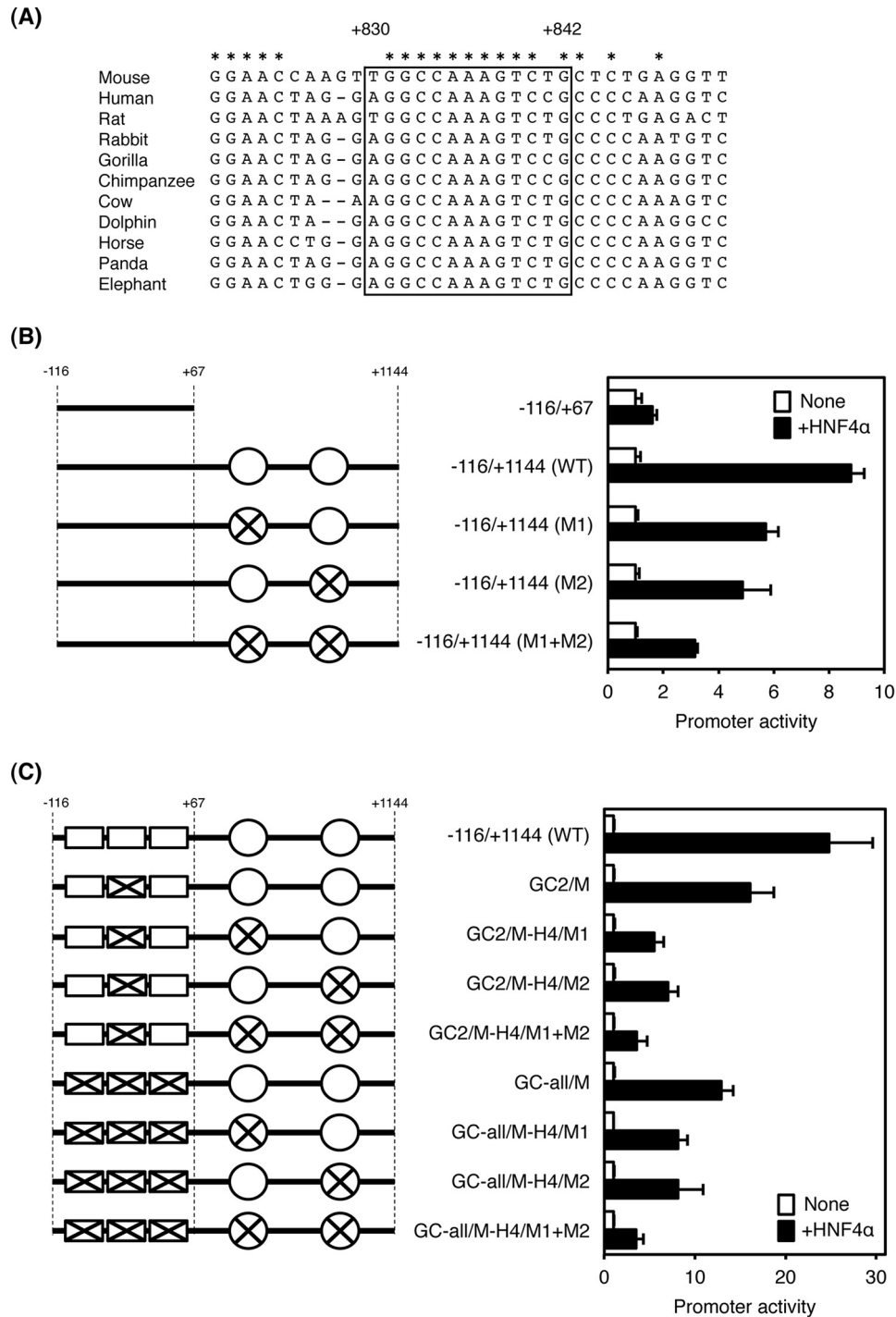


FIGURE 4. Requirement of the minimal promoter of the *Tfr2* gene for transactivation by HNF4 α . *A*, sequence alignment of the proximal promoter of the *Tfr2* gene in mouse, human, rat, rabbit, gorilla, chimpanzee, cow, dolphin, horse, panda, and elephant. Predicted HNF4 α -binding site is boxed. Completely conserved nucleotides among the species are shown by asterisks. *B*, mutations were introduced into the HNF4 α -binding sites in the proximal promoter of the *Tfr2* gene. Empty vector or HNF4 α expression vector was co-transfected with the mutated proximal promoter and the minimal distal promoter, and the enhancer activity was measured. *C*, mutations were introduced into the HNF4 α -binding sites and GC-rich sequences in the *Tfr2* promoter. Empty vector or HNF4 α expression vector was co-transfected with the mutated promoter, and the enhancer activity was measured. The normalized activity \pm S.D. ($n = 3$) is presented as promoter activity based on empty vector-transfected control.

exhibited elevated transferrin saturation (33), suggesting that absorption of iron from the duodenal FPN1 would be increased by reduced expression of *Hamp*. In contrast, *Hnf4a*^{ΔH} mice exhibited normal transferrin saturation. Thus, the phenotype of *Hnf4a*^{ΔH} mice does not overlap with those of liver-specific *Tfr2*-null mice, despite the fact that HNF4 α is an upstream

regulator of TFR2. A potential reason for this discrepancy is that lack of HNF4 α may have a profound effect on hepatic iron metabolism compared with that of TFR2.

This study further shows that HNF4 α binds and activates transcription of *Tfr2*. Previous studies showed that the mouse *Tfr2* proximal and distal promoter was transactivated in the

Regulation of *Tfr2* by Hepatic HNF4 α

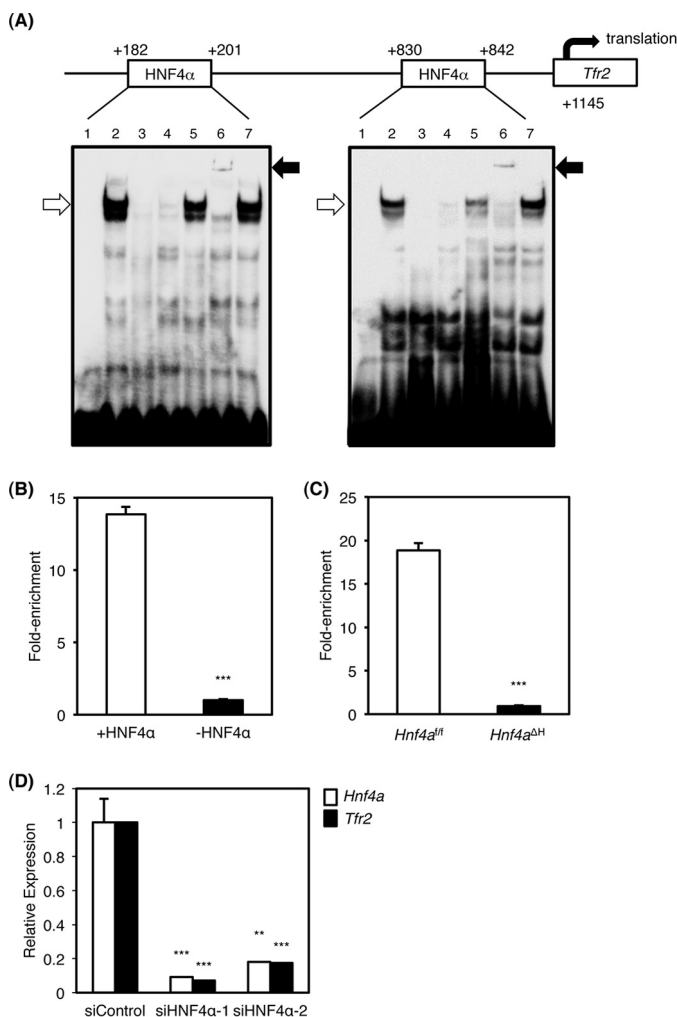


FIGURE 5. Identification of HNF4 α -binding sites in the *Tfr2* promoter and HNF4 α -dependent transactivation of the *Tfr2* gene. *A*, gel mobility shift analysis. Nuclear extracts from HepG2 cells were incubated with the probe carrying the distal (*left panel*) and proximal (*right panel*) HNF4 α -binding sites in the *Tfr2* promoter in the absence (*lane 2*) or presence of the unlabeled *Tfr2*, the *Otc*, and the mutated *Tfr2* probes (*lanes 3–5*). For supershift analysis, anti-HNF4 α and anti-PPAR α antibodies were added (*lanes 6 and 7*). *B*, chromatin immunoprecipitation using HepG2 cells were performed with anti-HNF4 α antibody and normal goat IgG. The regions with the proximal HNF4 α -binding sites (+HNF4 α) and the regions without HNF4 α -binding site (–HNF4 α) in the human *MIR-194/192* gene were amplified. The data from real time PCR were normalized relative to the input and expressed as fold-enrichment. ***, $p < 0.001$. *C*, chromatin immunoprecipitation using the livers of *Hnf4a* Δ H and *Hnf4a* Δ H/H mice with anti-HNF4 α antibody and normal goat IgG. The regions between the proximal and the distal HNF4 α -binding sites in the mouse *Tfr2* promoter and the regions without HNF4 α -binding site in the mouse *Hmgcs2* gene were amplified by real time PCR. The data were normalized relative to the input and expressed as fold-enrichment over data from the IgG control. ***, $p < 0.001$. *D*, 10 nM siRNA for HNF4 α (*siHNF4 α*) or negative control (*siControl*) was transfected into HepG2 cells. Real time PCR for HNF4 α (*white bar*) and *TFR2* mRNA (*black bar*) from total RNA of siRNA-transfected cells ($n = 3$) is shown. Data are mean \pm S.D. **, $p < 0.01$; ***, $p < 0.001$ compared with *siControl*-treated cells.

presence of GATA-1 and C/EBP α (27). Of these factors, GATA-1 would not be an essential factor to transactivate *Tfr2* in the liver because GATA-1 is a master regulator for erythroid differentiation and transactivates erythroid-specific genes (34, 35). Moreover, C/EBP α is enriched in the liver and positively regulates many liver-enriched genes (36). Although the expression of hepatic *Cebpa* was decreased by 45% in *Hnf4a* Δ H mice (37), no significant change of hepatic *Tfr2* mRNA expression

was detected in *Cebpa* Δ H mice. Additionally, the transactivation potential of C/EBP α alone for the *Tfr2* promoter without GATA-1 is much lower as compared with that with GATA-1 (27), and the contribution of C/EBP α to *Tfr2* regulation would be minor in the liver. Although details on transcriptional regulation of the *Tfr2* gene in the liver are not clear, HNF4 α could directly regulate the *Tfr2* expression through at least two HNF4 α -binding sites. Unlike the highly conserved binding site at +830/+842, the binding site at +182/+201 is not conserved among the species, and disruption of both binding sites did not completely inhibit the HNF4 α -dependent transactivation. However, HNF4 α knockdown greatly suppressed *TFR2* expression in human hepatoma cells, indicating that there might be additional HNF4 α -binding sites within the proximal promoter. This study revealed that GC-rich regions in the distal promoter were also important for maximal transactivation of the *Tfr2* gene promoter. It was reported that cooperation of the HNF4 α and GC-rich regions is important for transactivation of the human *APOC3* gene and mouse *Slc27a5* gene (38, 39), indicating that the GC-rich regions and the HNF4 α -binding sites in the *Tfr2* promoter can be the basal *cis*-elements and the liver-specific enhancer elements, respectively.

Although HNF4 α was found to directly regulate *Tfr2* expression, the mechanism for repressed expression of hepatic *Hamp* expression in *Hnf4a* Δ H mice could not be determined in this study. Because HNF4 α is a master regulator for maintenance of liver-specific functions and severe liver dysfunction and inflammation were actually observed in *Hnf4a* Δ H mice, the possibility cannot be excluded that complicated secondary effects would transactivate *Hamp* expression and lower the effect of reduced expression of *Tfr2* in *Hnf4a* Δ H mice. Despite the fact that *Tfr2* is a direct target for HNF4 α , remarkable changes of gene expression override the potential effects and phenotypes caused by decreased expression of *Tfr2* in *Hnf4a* Δ H mice. Consequently, HNF4 α is expected to transactivate *Hamp* through modulation of *Tfr2* expression in the normal liver.

In conclusion, hepatic HNF4 α significantly contributes to iron homeostasis and directly regulates *Tfr2* expression. Thus, augmentation of hepatic HNF4 α signaling could be of value for the treatment of hypoferrremia and anemia.

Author Contributions—S. M., M. O., Y. M., S. S., and T. F. conducted most of the experiments and analyzed the results. M. U. M. conducted experiments of IronChip analysis. M. T. and N. A. conducted experiments of real time PCR and ChIP analysis. H. O. and M. S. conducted experiments of siRNA. Y. I. conceived the idea for the project and wrote the paper with F. J. G.

Acknowledgments—We thank Prof. K. Wakamatsu for encouragement in the early phases of this work. We also acknowledge R. Yoshida for exploratory work on this project.

References

- Ganz, T. (2013) Systemic iron homeostasis. *Physiol. Rev.* **93**, 1721–1741
- Muñoz, M., García-Erce, J. A., and Remacha, A. F. (2011) Disorders of iron metabolism. Part 1: molecular basis of iron homeostasis. *J. Clin. Pathol.* **64**, 281–286
- Wang, J., and Pantopoulos, K. (2011) Regulation of cellular iron metabolism. *Biochem. J.* **434**, 365–381

4. Aisen, P. (2004) Transferrin receptor 1. *Int. J. Biochem. Cell Biol.* **36**, 2137–2143
5. Hayashi, A., Wada, Y., Suzuki, T., and Shimizu, A. (1993) Studies on familial hypotransferrinemia: unique clinical course and molecular pathology. *Am. J. Hum. Genet.* **53**, 201–213
6. Kawabata, H., Yang, R., Hiramata, T., Vuong, P. T., Kawano, S., Gombart, A. F., and Koeffler, H. P. (1999) Molecular cloning of transferrin receptor 2. A new member of the transferrin receptor-like family. *J. Biol. Chem.* **274**, 20826–20832
7. Camaschella, C., Roetto, A., Cali, A., De Gobbi, M., Garozzo, G., Carella, M., Majorano, N., Totaro, A., and Gasparini, P. (2000) The gene TFR2 is mutated in a new type of haemochromatosis mapping to 7q22. *Nat. Genet.* **25**, 14–15
8. West, A. P., Jr., Bennett, M. J., Sellers, V. M., Andrews, N. C., Enns, C. A., and Bjorkman, P. J. (2000) Comparison of the interactions of transferrin receptor and transferrin receptor 2 with transferrin and the hereditary hemochromatosis protein HFE. *J. Biol. Chem.* **275**, 38135–38138
9. Worthen, C. A., and Enns, C. A. (2014) The role of hepatic transferrin receptor 2 in the regulation of iron homeostasis in the body. *Front. Pharmacol.* **5**, 34
10. Gao, J., Chen, J., Kramer, M., Tsukamoto, H., Zhang, A. S., and Enns, C. A. (2009) Interaction of the hereditary hemochromatosis protein HFE with transferrin receptor 2 is required for transferrin-induced hepcidin expression. *Cell Metab.* **9**, 217–227
11. Nemeth, E., Tuttle, M. S., Powelson, J., Vaughn, M. B., Donovan, A., Ward, D. M., Ganz, T., and Kaplan, J. (2004) Hepcidin regulates cellular iron efflux by binding to ferroportin and inducing its internalization. *Science* **306**, 2090–2093
12. Yun, S., and Vincelette, N. D. (2015) Update on iron metabolism and molecular perspective of common genetic and acquired disorder, hemochromatosis. *Crit. Rev. Oncol. Hematol.* **95**, 12–25
13. Sladek, F. M., and Seidel, S. D. (2001) in *Nuclear Receptor and Genetic Disease* (Burris, T. P., and McCabe, E., eds) pp. 309–361, Academic Press, San Diego
14. Schrem, H., Klempnauer, J., and Borlak, J. (2002) Liver-enriched transcription factors in liver function and development. Part I: the hepatocyte nuclear factor network and liver-specific gene expression. *Pharmacol. Rev.* **54**, 129–158
15. Schaeffer, E., Guillou, F., Part, D., and Zakin, M. M. (1993) A different combination of transcription factors modulates the expression of the human transferrin promoter in liver and Sertoli cells. *J. Biol. Chem.* **268**, 23399–23408
16. Truksa, J., Lee, P., and Beutler, E. (2009) Two BMP responsive elements, STAT, and bZIP/HNF4/COUP motifs of the hepcidin promoter are critical for BMP, SMAD1, and HJV responsiveness. *Blood* **113**, 688–695
17. Courselaud, B., Pigeon, C., Inoue, Y., Inoue, J., Gonzalez, F. J., Leroyer, P., Gilot, D., Boudjema, K., Guguen-Guillouzo, C., Brissot, P., Loréal, O., and Ilyin, G. (2002) C/EBP α regulates hepatic transcription of hepcidin, an antimicrobial peptide and regulator of iron metabolism. *J. Biol. Chem.* **277**, 41163–41170
18. Hayhurst, G. P., Lee, Y. H., Lambert, G., Ward, J. M., and Gonzalez, F. J. (2001) Hepatocyte nuclear factor 4 α (nuclear receptor 2A1) is essential for maintenance of hepatic gene expression and lipid homeostasis. *Mol. Cell Biol.* **21**, 1393–1403
19. Inoue, Y., Hayhurst, G. P., Inoue, J., Mori, M., and Gonzalez, F. J. (2002) Defective ureagenesis in mice carrying a liver-specific disruption of hepatocyte nuclear factor 4 α (HNF4 α). HNF4 α regulates ornithine transcarbamylase *in vivo*. *J. Biol. Chem.* **277**, 25257–25265
20. Inoue, Y., Yu, A. M., Yim, S. H., Ma, X., Krausz, K. W., Inoue, J., Xiang, C. C., Brownstein, M. J., Eggertsen, G., Björkhem, I., and Gonzalez, F. J. (2006) Regulation of bile acid biosynthesis by hepatocyte nuclear factor 4 α . *J. Lipid Res.* **47**, 215–227
21. Inoue, Y., Inoue, J., Lambert, G., Yim, S. H., and Gonzalez, F. J. (2004) Disruption of hepatic C/EBP α results in impaired glucose tolerance and age-dependent hepatosteatosis. *J. Biol. Chem.* **279**, 44740–44748
22. Muckenthaler, M., Richter, A., Gunkel, N., Riedel, D., Polycarpou-Schwarz, M., Hentze, S., Falkenhahn, M., Stremmel, W., Ansorge, W., and Hentze, M. W. (2003) Relationships and distinctions in iron-regulatory networks responding to interrelated signals. *Blood* **101**, 3690–3698
23. Muckenthaler, M., Roy, C. N., Custodio, A. O., Miñana, B., deGraaf, J., Montross, L. K., Andrews, N. C., and Hentze, M. W. (2003) Regulatory defects in liver and intestine implicate abnormal hepcidin and Cybrd1 expression in mouse hemochromatosis. *Nat. Genet.* **34**, 102–107
24. Richter, A., Schwager, C., Hentze, S., Ansorge, W., Hentze, M. W., and Muckenthaler, M. (2002) Comparison of fluorescent tag DNA labeling methods used for expression analysis by DNA microarrays. *BioTechniques* **33**, 620–628
25. Bartnikas, T. B. (2012) Known and potential roles of transferrin in iron biology. *Biometals* **25**, 677–686
26. Bernstein, S. E. (1987) Hereditary hypotransferrinemia with hemosiderosis, a murine disorder resembling human atransferrinemia. *J. Lab. Clin. Med.* **110**, 690–705
27. Kawabata, H., Germain, R. S., Ikezoe, T., Tong, X., Green, E. M., Gombart, A. F., and Koeffler, H. P. (2001) Regulation of expression of murine transferrin receptor 2. *Blood* **98**, 1949–1954
28. Wallander, M. L., Leibold, E. A., and Eisenstein, R. S. (2006) Molecular control of vertebrate iron homeostasis by iron regulatory proteins. *Biochim. Biophys. Acta* **1763**, 668–689
29. Core, A. B., Canali, S., and Babitt, J. L. (2014) Hemojuvelin and bone morphogenetic protein (BMP) signaling in iron homeostasis. *Front. Pharmacol.* **5**, 104
30. Rolo, A. P., Teodoro, J. S., and Palmeira, C. M. (2012) Role of oxidative stress in the pathogenesis of nonalcoholic steatohepatitis. *Free Radic. Biol. Med.* **52**, 59–69
31. Handy, D. E., and Loscalzo, J. (2012) Redox regulation of mitochondrial function. *Antioxid. Redox Signal.* **16**, 1323–1367
32. Wallace, D. F., Summerville, L., Lusby, P. E., and Subramaniam, V. N. (2005) First phenotypic description of transferrin receptor 2 knockout mouse, and the role of hepcidin. *Gut* **54**, 980–986
33. Wallace, D. F., Summerville, L., and Subramaniam, V. N. (2007) Targeted disruption of the hepatic transferrin receptor 2 gene in mice leads to iron overload. *Gastroenterology* **132**, 301–310
34. Pevny, L., Simon, M. C., Robertson, E., Klein, W. H., Tsai, S. F., D'Agati, V., Orkin, S. H., and Costantini, F. (1991) Erythroid differentiation in chimeric mice blocked by a targeted mutation in the gene for transcription factor GATA-1. *Nature* **349**, 257–260
35. Welch, J. J., Watts, J. A., Vakoc, C. R., Yao, Y., Wang, H., Hardison, R. C., Blobel, G. A., Chodosh, L. A., and Weiss, M. J. (2004) Global regulation of erythroid gene expression by transcription factor GATA-1. *Blood* **104**, 3136–3147
36. Schrem, H., Klempnauer, J., and Borlak, J. (2004) Liver-enriched transcription factors in liver function and development. Part II: the C/EBPs and D site-binding protein in cell cycle control, carcinogenesis, circadian gene regulation, liver regeneration, apoptosis, and liver-specific gene regulation. *Pharmacol. Rev.* **56**, 291–330
37. Wiwi, C. A., Gupte, M., and Waxman, D. J. (2004) Sexually dimorphic P450 gene expression in liver-specific hepatocyte nuclear factor 4 α -deficient mice. *Mol. Endocrinol.* **18**, 1975–1987
38. Kardassis, D., Falvey, E., Tsantili, P., Hadzopoulou-Cladaras, M., and Zannis, V. (2002) Direct physical interactions between HNF-4 and Sp1 mediate synergistic transactivation of the apolipoprotein CIII promoter. *Biochemistry* **41**, 1217–1228
39. Inoue, Y., Yu, A. M., Inoue, J., and Gonzalez, F. J. (2004) Hepatocyte nuclear factor 4 α is a central regulator of bile acid conjugation. *J. Biol. Chem.* **279**, 2480–2489